3-HYDROXYANTHRALINIC ACID METABOLISM CONTROLS THE HEPATIC SREBP/LIPOPROTEIN AXIS, INHIBITS INFLAMMASOME ACTIVATION IN MACROPHAGES, AND DECREASES ATHEROSCLEROSIS IN *LDLR-/-* MICE

Running title: 3-HAA regulates SREBP and the inflammasome in atherosclerosis

Martin Berg[1]*, Konstantinos A Polyzos[1]*, Hanna Agardh[1], Roland Baumgartner[1], Maria J Forteza[1], Ilona Kareinen[1], Anton Gisterå[1], Gerhard Bottcher[3], Eva Hurt-Camejo[2], Göran K Hansson[1], Daniel FJ Ketelhuth[1]

Affiliations:

[1] Cardiovascular Medicine Unit, Center for Molecular Medicine, Department of Medicine, Karolinska Institute, and Karolinska University Hospital, SE-17176 Stockholm, Sweden

[2] Pathology, Drug Safety and Metabolism, IMED Biotech Unit, AstraZeneca, Gothenburg, Sweden

[3] Cardiovascular, Renal and Metabolic Diseases, Innovative Medicines and Early Development Biotech Unit, AstraZeneca, Sweden

* These authors contributed equally to this work.

***Word count*:** 3991

***Correspondence*:**

Daniel FJ Ketelhuth
Cardiovascular Research Unit
Center for Molecular Medicine, L8:03
Karolinska University Hospital
S-17176 Stockholm, Sweden
Fax: +46 8 313147
E-mail: daniel.ketelhuth@ki.se
Fax: +46 8 313147

ABSTRACT

Aims: Atherosclerosis is a chronic inflammatory disease involving immunological and metabolic processes. Metabolism of tryptophan (Trp) via the kynurenine pathway has shown immunomodulatory properties and the ability to modulate atherosclerosis. We identified 3-hydroxyanthranilic acid (3-HAA) as a key metabolite of Trp modulating vascular inflammation and lipid metabolism. The molecular mechanisms driven by 3-HAA in atherosclerosis have not been completely elucidated. In this study, we investigated whether two major signalling pathways, activation of SREBPs and inflammasome, are associated with the 3-HAA-dependent regulation of lipoprotein synthesis and inflammation in the atherogenesis process. Moreover, we examined whether inhibition of endogenous 3-HAA degradation affects hyperlipidaemia and atherosclerosis.

Methods and results: *In vitro*, we showed that 3-HAA reduces SREBP-2 expression and nuclear translocation, and apolipoprotein B secretion in HepG2 cell cultures, and inhibits inflammasome activation and IL-1β production by macrophages. Using *Ldlr-/-* mice, we showed that inhibition of 3-hydroxyanthranilic acid 3,4-dioxygenase (HAAO), which increases the endogenous levels of 3-HAA, decreases atherosclerosis and plasma lipids. Notably, HAAO inhibition led to decreased hepatic SREBP-2 mRNA levels and lipid accumulation, and improved liver pathology scores.

Conclusions: We discovered that the activity of SREBP-2 and the inflammasome can be regulated by 3-HAA metabolism. Moreover, our study highlights that targeting HAAO is a promising strategy to prevent and treat hypercholesterolemia and atherosclerosis.

INTRODUCTION

Ischaemic heart disease and stroke, the leading causes of death worldwide [1], are commonly caused by atherosclerosis, a chronic inflammatory disease affecting large- and medium-sized arteries. Atherosclerosis is initiated by the infiltration of low-density lipoprotein (LDL) across the endothelium, which subsequently becomes trapped and accumulates in the intima of the vessel [2]. Enzymatic and nonenzymatic modifications to the trapped LDL lead to the formation of danger-associated molecular patterns (DAMPs) that activate vascular and immune cells, triggering local inflammation [3].

Metabolism of tryptophan (Trp) via the kynurenine pathway has been linked to the inhibition of inflammation and the induction of immune tolerance [4]. Although expressed at basal levels in several tissues, the kynurenine pathway is tightly regulated and strongly induced in response to inflammation in many cell types, including endothelial cells, smooth muscle cells, and leukocytes in the vascular wall [5].

We have shown that Trp metabolism via the kynurenine pathway plays a protective role in the pathological process of atherosclerosis and identified 3-hydroxyanthranilic acid (3-HAA) as a major immunomodulatory metabolite that regulates vascular inflammation and plasma lipid levels [6-8]. However, the precise molecular mechanisms by which 3-HAA acts remain unclear.

Numerous experimental studies implicate inflammasome activation and interleukin 1-beta (IL-1β) secretion as key processes driving atherogenesis [9]. Recently, the Canakinumab Antiinflammatory Thrombosis Outcome Study (CANTOS) showed that blocking IL-1β is clinically relevant for treating atherosclerotic cardiovascular disease (CVD), as it significantly reduces the number of events and mortality [10, 11]. Interestingly, IL-1β has also been proposed to link inflammation with metabolic dysregulation [12].

Members of the sterol response element binding protein (SREBP or SREBF) transcription factor family function as principal regulators of lipid homeostasis, controlling lipid synthesis and catabolism [13]. IL-1β can increase SREBP-2 mRNA expression and nuclear translocation, which leads to increased intracellular cholesterol accumulation in HepG2 and primary hepatic cell cultures [14]. Conversely, recent studies have implicated both SREBP-1 and SREBP-2 in the regulation of IL-1β expression [15, 16].

In this study, we investigated whether the 3-HAA-driven effects on lipid levels and inflammation depend on the modulation of SREBPs and the inflammasome. Moreover, we evaluated whether 3-hydroxyanthranilic acid 3,4-dioxygenase (HAAO) inhibition, which increases endogenous 3-HAA levels, can modulate SREBPs, plasma lipids, and atherosclerosis in *Ldlr-/-* mice.

METHODS

HepG2 culture and treatments

The human hepatoma cell line HepG2 was purchased from ATCC (VA, USA) and cultured as previously described [17]. Briefly, cells were maintained in low glucose (1 g/l) Dulbecco's Modified Eagle's Medium (DMEM, Sigma Aldrich, MO, USA) supplemented with 10% foetal bovine serum (FBS), 2 mM L-glutamine, 100 units/ml penicillin and 100 µg/ml streptomycin (all from Gibco, UK). At least 14 days prior to the experiment, the cells were passaged, and the medium replaced with low glucose (1 g/l) DMEM supplemented with 2% AB+ human serum (Blodcentralen Karolinska Universitetssjukhuset, Sweden), 2 mM L-glutamine, 100 units/ml penicillin and 100 µg/ml streptomycin. Cells were treated overnight with increasing concentrations of 3-HAA (Sigma Aldrich, MO, USA), Phosphoinositide-dependent kinase-1 (PDK1) inhibitor KP372-1 (Sigma Aldrich, MO, USA), or vehicle according to the figure legends for gene and nuclear protein expression analysis, and immunofluorescence staining, or for 48 hours for apolipoprotein B (ApoB) secretion analysis. Medium of cells treated with KP372-1 was supplemented with high glucose (25 mM) and insulin (100 nM, Novo Nordisk, Denmark) during the treatment. 3-HAA and KP372-1 toxicity to HepG2 cells (Supplemental fig.1) was evaluated by PrestoBlue HS Cell Viability assay and LDH activity (both from Thermo, IL, USA) following the manufacturer's instructions.

Protein extraction, Western blotting and immunofluorescence staining

Nuclear proteins from treated HepG2 cells were extracted using the CelLytic Nuclear Extraction kit (Sigma Aldrich, Israel) according to the manufacturer's instructions. Total protein was extracted from bone marrow-derived macrophages with RIPA buffer. Arterial protein was extracted from frozen aortas of NCR-631-treated mice and PBS controls as previously described [18]. Protein concentration was measured with a DC protein reaction kit (BioRad, USA) or the Pierce 660 assay (Thermo, IL, USA) prior to Western blotting. After the gel electrophoresis of either nuclear extract from HepG2 cells, or treated mouse macrophages, or aortas, proteins were blotted on polyvinylidene difluoride (PVDF) membranes and probed with rabbit anti-human SREBP-2 (Novus, CO, USA), mouse anti-human Histone H4, rabbit anti-mouse caspase-1, and rabbit anti-mouse Vinculin (all Abcam, UK). The secondary antibodies IRDye© donkey anti-rabbit 800W and IRDye© goat anti-mouse 680W (Li-Cor, NE, USA) were used, and detection was carried out using an Odyssey CLx infrared detection system (Li-Cor, NE, USA).

Immunofluorescence staining was carried out on HepG2 cells grown on Falcon™ chamber slides (Fischer Scientific, PA, USA). 25 000 cells were added to each well, and slides were incubated in experimental medium supplemented with human serum as stated above. The cells were incubated for two weeks, and the growth medium was replaced regularly. One day prior to staining, cells were treated overnight with 3-HAA or vehicle, as stated in the figure legends. Cells were then washed with PBS, fixed with formaldehyde and methanol and stained with rabbit anti-human SREBP-2 (Novus, CO, USA); nuclei were stained with DAPI. The secondary antibody DyLight 594 horse anti-rabbit (Vector Laboratories, CA, USA) was used, and images were acquired on a Leica TCS SP5 confocal microscope system (Leica, Germany).

Apolipoprotein B secretion analysis

ApoB secretion from HepG2 cells was measured as previously described [17]. Briefly, depending on the cell batch, 2–4 million cells were seeded in 75 cm^2 cell culture flasks. Equal numbers of cells were always seeded in both the treatment flask and the corresponding control flask. Cells were grown for 14 days in experimental growth medium supplemented with human serum as stated above. At the

start of treatment, the growth medium was removed, and the cells were washed three times. The final wash was collected and retained for future reference. Serum-free Opti-MEM (Gibco, UK) supplemented with 100 µM 3-HAA or control vehicle was then added. Cells were treated for 48 hours, and the supernatant was then collected and concentrated by size using Amicon Ultra centrifugational units (Millipore, Ireland). The concentrate was fractionated using an FPLC system with a Superose 6 Increase column (GE Healthcare, Sweden) and tris-buffered saline (TBS) at a flow rate of 0.4 ml/minute. Fractions were collected in a 96-well microplate using a Foxy Jr fraction collector (Teledyne, NE, USA), and ApoB was detected by ELISA (Mabtech, Sweden).

Generation of mouse bone marrow-derived macrophages and inflammasome activation in vitro

Bone marrow cells were extracted from the femurs and tibias of C57Bl/6 mice, differentiated in medium (DMEM, 10% FCS, 50 U/ mL penicillin, 50 g/mL streptomycin, 1 mmol/L sodium pyruvate, 2 mmol/L l-glutamine) supplemented with 20% L929 supernatant for 7 days as previously described [19] and then counted and plated for experiments.

To measure IL-1β production based on inflammasome activation, two steps are required [20]. First, initial priming with LPS (Enzo Life Science, USA) was used to induce the production of pro-IL-1β and potentiate the inflammasome response. A second activating signal, ATP (Sigma Aldrich, MO, USA), was then used to induce assembly of the inflammasome complex, cleavage of caspase-1, and the release of mature IL-1β. Treatment with 3-HAA was performed either one hour before LPS or 30 minutes before ATP. Supernatant IL-1β was measured by ELISA according to the manufacturer's instructions (R&D Systems, MN, USA). Caspase 1 activation was evaluated by western blot as earlier described.

RNA analysis

RNA was isolated from HepG2 cells and mouse livers using the RNeasy kit (Qiagen, Hilden, Germany). After approving the quality of the RNA on a BioAnalyser (Agilent Technologies, Waldbronn, Germany), it was reverse transcribed with a High-Capacity RNA-to-cDNA™ Kit (Thermo, IL, USA) and amplified by real time-PCR using assay-on-demand primers and probes (Thermo, IL, USA) in an ABI 7700 Sequence Detector (Applied Biosystems, Foster City, CA, USA). Hypoxanthine guanidine ribonucleosyl transferase (HPRT) was used as housekeeping gene. The complete list of assay-on-demand primers and probes is provided in the Supplemental Table 1. Data were analysed based on the relative expression method with the formula $2^{-\Delta\Delta CT}$, where ΔΔCT = ΔCT (sample) – ΔCT (calibrator = average CT values of all samples within each group) and ΔCT is the average CT of the housekeeping genes subtracted from the CT of the target gene.

Animals and treatment

Male *Ldlr-/-* mice (B6.129S7-Ldlrtm1Her/J) were purchased from the Jackson Laboratory (Charles River Laboratories) and allowed to acclimatize for 4 weeks. At twelve weeks of age, the mice were fed a western diet (corn starch, cocoa butter, casein, glucose, sucrose, cellulose flour, minerals, and vitamins comprising 17.2% protein, 21% fat (62.9% saturated, 33.9 unsaturated, and 3.4% polyunsaturated), 0.15% cholesterol, 43% carbohydrates, 10% H2O, and 3.9% cellulose fibres; R638 Lantmännen, Sweden) *ad libitum*. NCR-631 (AstraZeneca, Sweden) or PBS was administered by intraperitoneal injection (200 mg/kg in PBS, ~5 mg/injection) three times per week for eight weeks. This dose was selected based on previous titration study showing dose-dependent increase in the 3-HAA plasma levels [21]. A group of mice receiving 3-HAA (Sigma Aldrich, MO; 200 mg/kg in PBS, ~5 mg/injection; prepared as described in [6]) was used as a reference group for atherosclerosis and plasma lipid analysis. Aortic arch lesion was used as a primary endpoint in the study. Descriptive data

of all animal experiments are provided in Supplemental tables 2-5. All animal experiments were performed in accordance with national guidelines and approved by the Stockholm Norra regional ethics board (N139-12; N28-15), which conform to the guidelines from Directive 2010/63/EU of the European Parliament on the protection of animals used for scientific purposes

Tissue collection, en face analysis of the aortic arch, and immunohistochemistry

At the end of treatment, mice were euthanized with CO_2. Blood was collected by cardiac puncture, and vascular perfusion was performed with sterile RNase-free PBS. After perfusion, heart and the aortic arch was dissected and preserved for lesion and immunohistochemistry analyses. The liver was dissected and snap-frozen or preserved in a 4% % Phosphate-buffered formaldehyde for histopathology analyses. *En face* lipid accumulation in the mouse aortic arch was determined using Sudan IV staining. Images were captured using a Leica DC480 camera connected to a Leica MZ6 stereo microscope (Leica, Wetzlar, Germany). The plaque area was calculated as the percentage of the total surface area of the aortic arch (not including branching vessels) using Image J software (NIH, Bethesda, USA). The plaque cell markers in sections of aortic roots was evaluated using primary antibodies against CD68 (AbD Serotec, Kidlington, UK) and CD4 (BD Biosciences, Franklin Lakes, NJ, USA) that were applied to acetone-fixed cryosections. Detection was performed using an ABC alkaline phosphatase kit (Vector Laboratories, Burlingame, CA, USA) as previously described [22, 23]. Immunohistochemical data was obtained using Qwin computerized analysis (Leica, Wetzlar, Germany) of stained sections. Samples that were compromised during processing or analysis were excluded from the study. For the assessment of plaques, samples were coded and the evaluation performed by trained persons, which were blinded to the treatment groups.

Plasma, liver lipid and faecal cholesterol analysis

Plasma cholesterol and triglycerides were measured using enzymatic colorimetric kits (Randox Lab. Ltd. Crumin, UK) according to the manufacturer's instructions. Upon sacrifice, a piece of the liver was snap-frozen. Liver lipids and faecal cholesterol were extracted from liver samples and dried faeces using the Folch method [24]. Mouse faeces were collected during 6h daytime. Briefly, one hundred mg liver tissue or three hundred mg dried and ground faeces were homogenized in methanol, and lipids were extracted by chloroform separation (methanol: chloroform (1:2). After drying, the extracts were redissolved in 1% Triton-100 and cholesterol and triglyceride content were measured using enzymatic colorimetric kits (Randox Lab. Ltd. Crumin, UK) according to the manufacturer's instructions.

Liver histopathology analysis and CD68 staining

Liver samples were fixed for 24-48 h in 4% buffered formaldehyde solution, dehydrated in a series of graded alcohol, and embedded in paraffin wax. Serial sections of 4 µm were rehydrated, and stained with hematoxylin-eosin (H&E) for light microscopy histopathological and immunostaining assessment. Histopathological examination and evaluation of liver tissue samples was performed on H&E stained sections and degree of steatosis and inflammation was scored on a semi quantitative 5 grade scale (0= normal; 1= minimal; 2= slight; 3= moderate; 4= marked; 5= severe) as previously described [25]. All histological assessments were performed by a trained pathologist who was blinded to the treatments. Hepatic macrophage number was evaluated using a primary antibody against Mac-2 antibody (Cedarlane Laboratories, Burlington, Canada) and detected by standard immunoperoxidase technique. Slides were examined by light microscopy and quantitative analysis carried out using at least 4 randomly selected fields from each section. Mean Mac-2+ cells/field for each mouse were used to plot graphs.

Lipoprotein turnover experiments

LDL clearance was determined by intravenous injection of fluorescein isothiocyanate (FITC) labelled LDL particles. FITC labelling was done as earlier described [26]. Mice were injected intravenously with 2.5 µg of LDL protein content per g of bodyweight and bled via the tail vein 1, 5, 10, 30 and 60 minutes post injection. Fluorescence in plasma was detected using a fluorescence plate reader (Perkin Elmer, USA), the results were corrected for haemoglobin by using a standard curve. VLDL production was assessed as earlier described [26]. Briefly, blood was collected via the tail vein before the start of the experiment. The mice then received an intraperitoneal injection of 500mg/kg body weight of Tyloxapol (Sigma Aldrich, MO, USA) to inhibit lipolysis. Blood was collected after 2 and 6 hours and the mice were euthanized. Triglyceride levels, as a measure of VLDL output, were determined using enzymatic colorimetric kit (Randox Lab. Ltd. Crumin, UK) according to the manufacturer's instructions.

Statistical analysis

The results are presented as the mean ± SEM if not otherwise stated. The Mann-Whitney U-test was used for comparison between two groups, and Kruskal-Wallis ANOVA with Dunn's post-test for comparisons between more than two groups. Correlations were calculated using Spearman's rank test. P-values <0.05 were considered significant.

RESULTS

3-HAA regulates the SREBP/lipoprotein axis in HepG2 cells

HepG2 cell cultures were used to study the direct effects of 3-HAA on *SREBP* mRNA levels, SREBP-2 translocation to the nucleus, and ApoB secretion. 3-HAA treatment led to a significant dose-dependent decrease in SREBP-2 mRNA expression (fig. 1A), while SREBP-1 mRNA was not significantly affected. Notably, upon insulin and glucose challenge, which is known to stimulate SREBP-1 expression [27], 3-HAA treatment also influenced SREBP-1 mRNA levels (Supplemental fig. 2). Interestingly, inhibition of PDK1, which has been suggested to mediate 3-HAA anti-inflammatory effects in T cells [28], also reduced SREBP-2 mRNA levels in HepG2 cells (Supplemental fig.3)

Western blot analysis of nuclear extracts from HepG2 cells revealed that 3-HAA substantially reduced cleaved SREBP-2 protein levels in the nucleus (fig. 1B), which was further confirmed by immunofluorescence staining (fig. 1C). Next, we evaluated whether 3-HAA-driven effects on SREBP could influence lipoprotein secretion *in vitro*. The ApoB levels in the supernatant of 3-HAA treated cells were reduced by approximately 47% compared to controls (fig. 1D).

3-HAA inhibits inflammasome activation and IL-1β secretion by macrophages

Bone marrow-derived macrophages from C57BL/6J mice were used to investigate whether 3-HAA modulates the inflammasome activation. The effects of 3-HAA on both inflammasome priming and activation were investigated. Treatment with 3-HAA before LPS-priming reduced IL-1β secretion in a dose-dependent manner (fig. 2A). Interestingly, treatment with 3-HAA shortly before ATP stimulation showed very similar effects on the inhibition of IL-1β (fig. 2B). Corroborating these findings, we observed a dose-dependent decrease in cleaved caspase-1 protein in macrophages treated with 3-HAA before LPS (fig. 2C). A decrease in cleaved caspase-1 was also observed at the highest 3-HAA dose when added before ATP (fig. 2C).

HAAO blockade reduces the atherosclerotic lesion burden and plasma lipids

Treatment of *Ldlr-/-* mice with the HAAO inhibitor NCR-631 (fig. 3A) decreased the atherosclerotic lesion area in the aortic arch by approximately 50% compared to PBS control mice (fig. 3B). The reduction in the lesion area was comparable to that induced by exogenous 3-HAA administration, which was used as a reference. Treatment with NCR-631 also led to reduced plasma levels of total cholesterol (fig. 3C) and triglycerides (fig. 3D) compared to those in the PBS controls, and were similar to 3-HAA treatment. No difference in body weight was observed between the treatment groups (fig. 3E).

HAAO blockade effects on vascular inflammation

We evaluated whether NCR-631 could influence plaque CD68 macrophage and CD4+ T-cell infiltration in the plaque. Despite the significant effects of NCR-631 in plaque area, no differences in the percentage of macrophages and CD4+ T cells were observed (fig. 4A-B). Although this could sound surprising, it is in line with our previous finding that IDO inhibition, which reduces 3-HAA endogenous levels, accelerated atherosclerosis despite showing no changes in plaque cellular composition [7].

Because 3-HAA modulated the inflammasome activation *in vitro*, we investigated whether this pathway was influenced *in vivo* upon increased levels of endogenous 3-HAA due to HAAO blockade. Indeed, a significant decrease in pro-caspase-1, and a trend decrease in cleaved caspase-1 were observed in aortic protein extracts from NCR-631 treated mice compared to PBS controls (fig. 4C).

NCR-631 treatment reduces hepatic SREBP-2 mRNA levels, improves liver histopathological scores, and decreases liver lipid accumulation

We demonstrated that 3-HAA regulates the SREBP mRNA levels in HepG2 cell cultures. HAAO blockade *in vivo* with NCR-631, known to increase endogenous 3-HAA levels [21], led to decreased hepatic SREBP-2 mRNA levels compared to PBS-treated controls (fig. 5A). The mRNA expression of one of its major target gene, 3-hydroxy-3-methylglutaryl-CoA reductase (HMGCR), was also decreased by NCR-631 treatment (fig. 5B). NCR-631 treatment exerted no effect on hepatic SREBP-1 or its target gene stearoyl-CoA desaturase 1 (SCD-1) mRNA expression (fig. 5C and D). Interestingly, a positive correlation between hepatic macrophage infiltration and Srebf2, and Hmgcr was observed in our mouse model (Supplemental fig. 4).

Histopathological examination and semiquantitative scoring of the prepared liver samples revealed a reduction in steatosis grade as well as lobular inflammation and hepatocyte ballooning-like degeneration in mice treated with NCR-631 (fig. 45 and F). In line with these data, HAAO blockade led to reduced hepatic cholesterol and triglyceride levels (fig.5 G-H) as well as reduced faecal cholesterol levels (Supplemental fig. 5). These findings are consistent with the *in vitro* data obtained from HepG2 cells, supporting the protective potential of 3-HAA in the liver.

Effects of NCR-631 treatment on lipoproteins turnover

In order to investigate whether HAAO blockade influences lipoprotein clearance *in vivo,* we injected FITC-labelled LDL into *Ldlr-/-* mice that were treated with PBS or NCR-631 for 8 weeks. No significant difference in the clearance of LDL was observed between treatments (fig. 6A). In order to further elucidate the mechanisms underlying the hypolipidemic effects of NCR-631, mice were injected with tyloxapol that blocks lipolysis, allowing the measurement of VLDL secretion. In line with our in vitro data, NCR-631 treated mice presented a 24% lower triglyceride levels after six hours of tyloxapol injection, reflecting a reduced VLDL output (fig. 6B).

DISCUSSION

In this study, we demonstrate that 3-HAA inhibits signalling mediated by the master regulator of cholesterol synthesis in the liver, SREBP-2. We also show that 3-HAA inhibits inflammasome activation and IL-1β production in macrophages. By pharmacologically blocking HAAO, we show that the *in vivo* metabolism of 3-HAA affects the SREBP-2/lipoprotein axis and atherosclerosis in *Ldlr-/-* mice.

Inflammation is a key regulatory process that links multiple CVD risk factors, especially metabolic alterations, including dyslipidaemia, diabetes, obesity, and fatty liver disease [29]. Interestingly, alterations in the metabolism of Trp have been shown to influence plasma lipoprotein and glucose levels, obesity, and cardiovascular clinical outcomes [4, 5].

The Trp metabolite 3-HAA is a pronounced antiinflammatory molecule generated by the kynurenine pathway. It can control cytokine secretion by immune cells and induce regulatory T cell differentiation [30, 31]. Despite numerous reports indicating a protective effect against inflammation in preclinical models of disease, e.g., experimental autoimmune encephalomyelitis [30], asthma [28], and transplantation [32], little is known about 3-HAA-mediated intracellular signals. No specific molecular mechanisms driven by 3-HAA in the liver have been reported.

SREBPs are transcription factors that control the biosynthesis of cholesterol, fatty acids, and triglycerides [33]. The transcription, expression, and activation of SREBPs can be regulated by different stimuli, including nutritional status, hormones, and stress [34]. In the nucleus, SREBPs regulate the transcription of enzymes involved in lipid biosynthesis, including HMGCR and SCD-1 [13, 35].

Changes in Intracellular cholesterol levels drive SREBP-2 expression and nuclear translocation, leading to gene transcription and increased cholesterol synthesis. In our study, Srebf2 is found downregulated in livers from NCR-631 treated mice, despite having lower plasma and hepatic lipid levels. Taking into account that lower cholesterol levels should stimulate Srebf2 expression and activation, and the fact that we show 3-HAA directly inhibits SREBP-2 mRNA and protein levels in HepG2 cultures, our present study provides the first evidence that SREBP-2 can be transcriptionally regulated by a Trp metabolite–this also leads to reduced SREBP-2 nuclear translocation. Whether 3-HAA has a direct effect on SREBP-2 nuclear translocation requires further investigation. Decreased SREBP-2 activity should lead to decreased LDL receptor expression, which could negatively influence plasma cholesterol levels [36]. A limitation of our study, potential effects on LDLr could not be taken into consideration in our experimental atherosclerosis model using *Ldlr-/-* mice.

The antiinflammatory effects of 3-HAA may involve inhibition of the PDK1, NF-κB, and p38/c-Jun pathways [28, 37]. Our study extends the list of target pathways and identifies 3-HAA as a potent regulator of the inflammasome. In our study, LPS was used to upregulate NACHT, LRR and PYD domain-containing protein 3 (NLRP3) and pro-IL-1β expression, while ATP stimulation was used to activate NLRP3 inflammasome assembly. Considering that we and others have shown that 3-HAA inhibits NF-κB-mediated responses [6, 38], for example the secretion of pro-inflammatory cytokines and chemokines by macrophages, this could be implied as the main mechanism influencing IL-1β secretion. However, the fact that 3-HAA impairs IL-1β secretion from macrophages regardless of whether it is administered before LPS-priming or shortly before inflammasome activation suggests that 3-HAA major effect is on NLRP3 inflammasome complex assembly. Reduced levels of cleaved caspase-1 protein in macrophages treated with 3-HAA for thirty minutes before ATP stimulation strengthen this hypothesis. How 3-HAA acutely inhibits inflammasome assembly remains undiscovered. ATP-induced purinergic signalling has been implicated as a major inducer of NLRP3 inflammasome complex assembly [39]. It will be interesting to test whether 3-HAA effects on IL-1β occur through downstream signals from such receptors, e.g. P2X7.

Preclinical studies have shown that inhibition of kynurenine pathway enzymes may be a suitable strategy for treating cancer and neuropsychiatric disorders [40]. Interestingly, *in vivo* targeting of HAAO has shown neuroprotective effects [21], including reducing LPS- and IL-1β-induced neuroinflammation [41]. Here, we show that blocking HAAO leads to a significant reduction in atherosclerosis and plasma lipid levels, resembling the effects of exogenous 3-HAA administration. Despite not affecting lesion cell composition, our data suggest that inflammasome activation in the artery wall is also impaired by HAAO inhibition, which goes in line with our in vitro experiments with 3-HAA. Altogether, our data identify HAAO as a potential therapeutic target, and strengthen the concept that manipulation of Trp metabolism via the kynurenine pathway can be used to treat and prevent atherosclerotic CVDs.

SREBP-2 inhibition can reduce plasma and tissue lipid levels, increase insulin sensitivity, reduce atherosclerosis and increase plaque stability in *Ldlr-/-* mice [42]. Our mice treated with NCR-631 showed a clear improvement in liver histopathological scores as well as low plasma lipid levels and hepatic lipid deposition. These findings together with the *in vitro* data from HepG2 cell cultures indicate that increased levels of 3-HAA regulate SREBP-2 and HMGCR expression in the liver. Taking into account that NCR-631 had no effects on lipoprotein clearance and decreased hepatic VLDL output, our data support the notion that increased endogenous levels of 3-HAA affect the cholesterol synthetic pathway rather than its catabolism. Reduced faecal cholesterol in NCR-631-treated mice, reflecting lower hepatic and plasma cholesterol levels, further support this hypothesis. Altogether, our findings suggest that modulation of the SREBP/lipoprotein axis is a major atheroprotective effect of 3-HAA.

Fatty acid biosynthesis is regulated by activation of the SPREBP-1 pathway [43]. No major effects on SREBP-1 were observed in either 3-HAA-treated HepG2 cells or in the livers of NCR-631-treated mice. Nevertheless, an inhibitory effect of 3-HAA on SREBP-1 mRNA expression was observed in HepG2 cells treated with high glucose and insulin, known inducers of SREBP-1 [34]. Considering that chronic exposure to a high-fat diet can lead to changes in insulin sensitivity and type 2 diabetes, 3-HAA may potentially exerts atheroprotective effects that are mediated by SREPB-1 inhibition. This warrants further research.

Overexpression of SREBP-2 has been identified as a key feature of non-alcoholic steatohepatitis (NASH) [44, 45]. Thus, our data raise the notion that 3-HAA could have beneficial effects on other diseases, including the large spectrum of liver diseases ranging from steatosis to NASH, which is regarded as the hepatic component related to the metabolic syndrome and associated with an increased risk of developing CVD [46]. Downregulation of SREBP-2 has been suggested to inhibit IL-1β transcription [16]. Moreover, vascular activation of SREBP-2 has been implicated in NLRP3 inflammasome activation and atherosclerosis susceptibility [47]. The questions of whether 3-HAA metabolism can influence SREBP-2-dependent inflammasome activation and whether this metabolite is involved in hepatic disorders will be addressed in future studies.

In conclusion, we have identified two major signalling pathways modulated by 3-HAA, the SREBP-2/lipoprotein axis and inflammasome activation, both of which are linked to the regulation of inflammation during atherogenesis. Furthermore, our study identifies HAAO as a potential target for treating hypercholesterolemia and atherosclerosis. Based on our study, strategies that lead to increased endogenous levels of 3-HAA may have high therapeutic potential for the prevention and treatment of atherosclerotic CVDs.

FUNDING

This study was partially funded by a research collaboration grant from AstraZeneca. This work was also supported by the Swedish Heart-Lung Foundation, the Novo Nordisk Foundation (NNF15CC0018346), the Karolinska Institute Cardiovascular Program Young investigator Career Development Grant, the CERIC Linnaeus Program (349-2007-8703), the Swedish Research Council-Medicine (2016-02738), the Stockholm County Council (ALF), and the European Union's Seventh Framework Programme [FP7/2007-2013] under grant agreements VIA (n° 603131, the VIA project is also supported by Academic and SME partners), Molstroke, and AtheroRemo. KAP is supported by the Alexander S. Onassis Foundation.

ACKNOWLEDGEMENTS

We thank Anneli Olsson, Ingrid Törnberg, and Linda Haglund for their technical assistance. We thank the AKM Animal Facility staff for their help with animal treatments. We thank Mohsen Karimi Arzenani for the anti-histone 4 monoclonal antibody. We thank Felipe Beccaria Casagrande for the assistance with western blots.

CONFLICTS OF INTEREST

DFJK and GKH hold patents on the use of 3-HAA for the prevention and treatment of hyperlipidaemia and its complications. The remaining authors have no disclosures to report. EHC and GB are full-time employees of AstraZeneca.

REFERENCES

1. Mathers CD, Boerma T, Ma Fat D. Global and regional causes of death. *Br Med Bull* 2009;**92**:7-32.
2. Tabas I, Williams KJ, Boren J. Subendothelial lipoprotein retention as the initiating process in atherosclerosis: update and therapeutic implications. *Circulation* 2007;**116**:1832-44.
3. Ketelhuth DF, Hansson GK. Modulation of autoimmunity and atherosclerosis - common targets and promising translational approaches against disease. *Circ J* 2015;**79**:924-33.
4. Baumgartner R, Forteza MJ, Ketelhuth DFJ. The interplay between cytokines and the Kynurenine pathway in inflammation and atherosclerosis. *Cytokine* 2017; S1043-4666(17)30259-4.
5. Polyzos KA, Ketelhuth DF. The role of the kynurenine pathway of tryptophan metabolism in cardiovascular disease. An emerging field. *Hamostaseologie* 2015;**35**.
6. Zhang L, Ovchinnikova O, Jonsson A, Lundberg AM, Berg M, Hansson GK, Ketelhuth DF. The tryptophan metabolite 3-hydroxyanthranilic acid lowers plasma lipids and decreases atherosclerosis in hypercholesterolaemic mice. *Eur Heart J* 2012;**33**:2025-34.
7. Polyzos KA, Ovchinnikova O, Berg M, Baumgartner R, Agardh H, Pirault J, Gistera A, Assinger A, Laguna Fernandez A, Back M, Hansson GK, Ketelhuth DF. Inhibition of indoleamine 2,3-dioxygenase (IDO) promotes vascular inflammation and increases atherosclerosis in Apoe-/- mice. *Cardiovasc Res* 2015;**106**:295-302
8. Ketelhuth DFJ. The immunometabolic role of indoleamine 2 3-dioxygenase in atherosclerotic cardiovascular disease: immune homeostatic mechanisms in the artery wall. *Cardiovasc Res* 2019;**115**:1408-1415
9. Libby P. Interleukin-1 Beta as a Target for Atherosclerosis Therapy: Biological Basis of CANTOS and Beyond. *J Am Coll Cardiol* 2017;**70**:2278-2289.
10. Ridker PM, Everett BM, Thuren T, MacFadyen JG, Chang WH, Ballantyne C, Fonseca F, Nicolau J, Koenig W, Anker SD, Kastelein JJP, Cornel JH, Pais P, Pella D, Genest J, Cifkova R, Lorenzatti A, Forster T, Kobalava Z, Vida-Simiti L, Flather M, Shimokawa H, Ogawa H, Dellborg M, Rossi PRF, Troquay RPT, Libby P, Glynn RJ, Group CT. Antiinflammatory Therapy with Canakinumab for Atherosclerotic Disease. *N Engl J Med* 2017;**377**:1119-1131.
11. Ridker PM, MacFadyen JG, Everett BM, Libby P, Thuren T, Glynn RJ, Grp CT. Relationship of C-reactive protein reduction to cardiovascular event reduction following treatment with canakinumab: a secondary analysis from the CANTOS randomised controlled trial. *Lancet* 2018;**391**:319-328.
12. Esser N, Legrand-Poels S, Piette J, Scheen AJ, Paquot N. Inflammation as a link between obesity, metabolic syndrome and type 2 diabetes. *Diabetes Res Clin Pract* 2014;**105**:141-50.
13. Brown MS, Goldstein JL. The SREBP Pathway: Regulation of Cholesterol Metabolism by Proteolysis of a Membrane-Bound Transcription Factor. *Cell* 1998;**89**:331-340.
14. Ma KL, Ruan XZ, Powis SH, Chen Y, Moorhead JF, Varghese Z. Inflammatory stress exacerbates lipid accumulation in hepatic cells and fatty livers of apolipoprotein E knockout mice. *Hepatology* 2008;**48**:770-81.
15. Im SS, Yousef L, Blaschitz C, Liu JZ, Edwards RA, Young SG, Raffatellu M, Osborne TF. Linking lipid metabolism to the innate immune response in macrophages through sterol regulatory element binding protein-1a. *Cell Metab* 2011;**13**:540-9.
16. Reboldi A, Dang EV, McDonald JG, Liang G, Russell DW, Cyster JG. 25-Hydroxycholesterol suppresses interleukin 1 driven inflammation downstream of type I interferon. *Science* 2014;**345**.
17. Pramfalk C, Larsson L, Hardfeldt J, Eriksson M, Parini P. Culturing of HepG2 cells with human serum improve their functionality and suitability in studies of lipid metabolism. *Biochim Biophys Acta* 2016;**1861**:51-9.
18. Forteza MJ, Polyzos KA, Baumgartner R, Suur BE, Mussbacher M, Johansson DK, Hermansson A, Hansson GK, Ketelhuth DFJ. Activation of the Regulatory T-Cell/Indoleamine 2,3-Dioxygenase Axis Reduces Vascular Inflammation and Atherosclerosis in Hyperlipidemic Mice. *Front Immunol* 2018;**9**:950.

19. Mills EL, Ryan DG, Prag HA, Dikovskaya D, Menon D, Zaslona Z, Jedrychowski MP, Costa ASH, Higgins M, Hams E, Szpyt J, Runtsch MC, King MS, McGouran JF, Fischer R, Kessler BM, McGettrick AF, Hughes MM, Carroll RG, Booty LM, Knatko EV, Meakin PJ, Ashford MLJ, Modis LK, Brunori G, Sevin DC, Fallon PG, Caldwell ST, Kunji ERS, Chouchani ET, Frezza C, Dinkova-Kostova AT, Hartley RC, Murphy MP, O'Neill LA. Itaconate is an anti-inflammatory metabolite that activates Nrf2 via alkylation of KEAP1. *Nature* 2018;**556**:113-117.
20. Schroder K, Tschopp J. The inflammasomes. *Cell* 2010;**140**:821-32.
21. Fornstedt-Wallin B, Lundstrom J, Fredriksson G, Schwarcz R, Luthman J. 3-Hydroxyanthranilic acid accumulation following administration of the 3-hydroxyanthranilic acid 3,4-dioxygenase inhibitor NCR-631. *Eur J Pharmacol* 1999;**386**:15-24.
22. Gistera A, Ketelhuth DF. Immunostaining of Lymphocytes in Mouse Atherosclerotic Plaque. *Methods Mol Biol* 2015;**1339**:149-59.
23. Puccetti P, Fallarino F, Italiano A, Soubeyran I, MacGrogan G, Debled M, Velasco V, Bodet D, Eimer S, Veldhoen M, Prendergast GC, Platten M, Bessede A, Guillemin GJ. Accumulation of an endogenous tryptophan-derived metabolite in colorectal and breast cancers. *PLoS One* 2015;**10**:e0122046.
24. Folch J, Lees M, Sloane Stanley GH. A simple method for the isolation and purification of total lipides from animal tissues. *J Biol Chem* 1957;**226**:497-509.
25. Bjursell M, Xu X, Admyre T, Bottcher G, Lundin S, Nilsson R, Stone VM, Morgan NG, Lam YY, Storlien LH, Linden D, Smith DM, Bohlooly YM, Oscarsson J. The beneficial effects of n-3 polyunsaturated fatty acids on diet induced obesity and impaired glucose control do not require Gpr120. *PLoS One* 2014;**9**:e114942.
26. Klingenberg R, Gerdes N, Badeau RM, Gistera A, Strodthoff D, Ketelhuth DF, Lundberg AM, Rudling M, Nilsson SK, Olivecrona G, Zoller S, Lohmann C, Luscher TF, Jauhiainen M, Sparwasser T, Hansson GK. Depletion of FOXP3+ regulatory T cells promotes hypercholesterolemia and atherosclerosis. *J Clin Invest* 2013; **123**:1323-34.
27. Kim JB, Sarraf P, Wright M, Yao KM, Mueller E, Solanes G, Lowell BB, Spiegelman BM. Nutritional and insulin regulation of fatty acid synthetase and leptin gene expression through ADD1/SREBP1. *J Clin Invest* 1998;**101**:1-9.
28. Hayashi T, Mo J-H, Gong X, Rossetto C, Jang A, Beck L, Elliott GI, Kufareva I, Abagyan R, Broide DH, Lee J, Raz E. 3-Hydroxyanthranilic acid inhibits PDK1 activation and suppresses experimental asthma by inducing T cell apoptosis. *Proc. Natl. Acad. Sci. USA* 2007;**104**:18619-18624.
29. van Diepen JA, Berbée JFP, Havekes LM, Rensen PCN. Interactions between inflammation and lipid metabolism: Relevance for efficacy of anti-inflammatory drugs in the treatment of atherosclerosis. *Atherosclerosis* 2013;**228**:306-315.
30. Yan Y, Zhang G-X, Gran B, Fallarino F, Yu S, Li H, Cullimore ML, Rostami A, Xu H. IDO upregulates regulatory T cells via tryptophan catabolite and suppresses encephalitogenic T cell responses in experimental autoimmune encephalomyelitis. *J. Immunol.* 2010;**185**:5953-5961.
31. Sharma MD, Huang L, Choi J-H, Lee E-J, Wilson JM, Lemos H, Pan F, Blazar BR, Pardoll DM, Mellor AL, Shi H, Munn DH. An Inherently Bifunctional Subset of Foxp3+ T Helper Cells Is Controlled by the Transcription Factor Eos. *Immunity* 2013;**38**:998-1012.
32. Fallarino F, Grohmann U, Vacca C, Bianchi R, Orabona C, Spreca A, Fioretti MC, Puccetti P. T cell apoptosis by tryptophan catabolism. *Cell Death Diff.* 2002;**9**:1069-1077.
33. Goldstein JL, DeBose-Boyd RA, Brown MS. Protein sensors for membrane sterols. *Cell* 2006;**124**:35-46.
34. Shimano H, Sato R. SREBP-regulated lipid metabolism: convergent physiology - divergent pathophysiology. *Nat Rev Endocrinol* 2017;**13**:710-730.
35. Horton JD, Shah NA, Warrington JA, Anderson NN, Park SW, Brown MS, Goldstein JL. Combined analysis of oligonucleotide microarray data from transgenic and knockout mice identifies direct SREBP target genes. *Proc Natl Acad Sci U S A* 2003;**100**:12027-32.
36. Brown MS, Goldstein JL. The SREBP pathway: regulation of cholesterol metabolism by proteolysis of a membrane-bound transcription factor. *Cell* 1997;**89**:331-40.

37. Lee W-S, Lee S-M, Kim M-K, Park S-G, Choi I-W, Choi I, Joo Y-D, Park S-J, Kang S-W, Seo S-K. The tryptophan metabolite 3-hydroxyanthranilic acid suppresses T cell responses by inhibiting dendritic cell activation. *Int. Immunopharmacol.* 2013;**17**:721-726.
38. Lee K, Kwak JH, Pyo S. Inhibition of LPS-induced inflammatory mediators by 3-hydroxyanthranilic acid in macrophages through suppression of PI3K/NF-kappaB signaling pathways. *Food Funct* 2016;**7**:3073-82.
39. Di Virgilio F. Liaisons dangereuses: P2X(7) and the inflammasome. *Trends Pharmacol Sci* 2007;**28**:465-72.
40. Fujigaki H, Yamamoto Y, Saito K. L-Tryptophan-kynurenine pathway enzymes are therapeutic target for neuropsychiatric diseases: Focus on cell type differences. *Neuropharmacology* 2016.
41. Luthman J, Radesäter A, Oberg C. Effects of the 3-hydroxyanthranilic acid analogue NCR-631 on anoxia-, IL-lfl- and LPS-induced hippocampal pyramidal cell loss in vitro. *Amino Acids* 1998;**14**:263-9.
42. Tang JJ, Li JG, Qi W, Qiu WW, Li PS, Li BL, Song BL. Inhibition of SREBP by a small molecule, betulin, improves hyperlipidemia and insulin resistance and reduces atherosclerotic plaques. *Cell Metab* 2011;**13**:44-56.
43. Amemiya-Kudo M, Shimano H, Hasty AH, Yahagi N, Yoshikawa T, Matsuzaka T, Okazaki H, Tamura Y, Iizuka Y, Ohashi K, Osuga J, Harada K, Gotoda T, Sato R, Kimura S, Ishibashi S, Yamada N. Transcriptional activities of nuclear SREBP-1a, -1c, and -2 to different target promoters of lipogenic and cholesterogenic genes. *J Lipid Res* 2002;**43**:1220-35.
44. Min HK, Kapoor A, Fuchs M, Mirshahi F, Zhou H, Maher J, Kellum J, Warnick R, Contos MJ, Sanyal AJ. Increased hepatic synthesis and dysregulation of cholesterol metabolism is associated with the severity of nonalcoholic fatty liver disease. *Cell Metab* 2012;**15**:665-74.
45. Caballero F, Fernandez A, De Lacy AM, Fernandez-Checa JC, Caballeria J, Garcia-Ruiz C. Enhanced free cholesterol, SREBP-2 and StAR expression in human NASH. *J Hepatol* 2009;**50**:789-96.
46. Anstee QM, Targher G, Day CP. Progression of NAFLD to diabetes mellitus, cardiovascular disease or cirrhosis. *Nat Rev Gastroenterol Hepatol* 2013;**10**:330-44.
47. Xiao H, Lu M, Lin TY, Chen Z, Chen G, Wang WC, Marin T, Shentu TP, Wen L, Gongol B, Sun W, Liang X, Chen J, Huang HD, Pedra JH, Johnson DA, Shyy JY. Sterol regulatory element binding protein 2 activation of NLRP3 inflammasome in endothelium mediates hemodynamic-induced atherosclerosis susceptibility. *Circulation* 2013;**128**:632-42.

FIGURE LEGENDS

Figure 1. 3-HAA reduces SREBP-2 expression and activity in HepG2 cells

Hepatocytes from the human hepatoma cell line HepG2 were treated overnight with different doses of 3-HAA. (A) SREBP-1 and SREBP-2 mRNA expression (pooled data from six independent experiments (duplicate wells). * P<0.05; Kruskal-Wallis ANOVA with Dunn's post-test. (B) Representative Western blot analysis of SREBP-2 in nuclear protein extracts; histone H4 was used as a loading control (top graph depicts SREBP-2/histone H4 band density ratios). (C) immunofluorescence staining of SREBP-2 (red); nuclear DAPI staining is shown in blue. (D) ApoB levels in supernatant of HepG2 cells; left panel, representative Superose 6 profile; right panel, area under the curve as percentage of controls (control n=5, 3-HAA n=6). AUC, area under the curve. ** P<0.01; Mann-Whitney U-test.

Figure 2. 3-HAA treatment inhibits the inflammasome in mouse macrophages

Mouse bone marrow-derived macrophages were treated with increasing concentrations of 3-HAA. Macrophages were primed with 10 ng/ml LPS for 6 hours, and the inflammasome was then activated with 1 mM ATP. Graphs show IL-1β secretion from cells treated with 3-HAA (A) 0.5 hour before LPS (n= differentiated cells from 7 individual mice, treated in duplicates) or (B) 30 min before ATP activation (n= differentiated cells from 5 individual mice, treated in duplicate). **P<0.01, **** P<0.0001; Kruskal-Wallis ANOVA with Dunn's post-test. (C) Representative western blot analysis of cleaved caspase-1 upon treatment with increasing doses of 3-HAA before LPS-priming, except one sample treated before ATP (denoted by §). Vinculin was used as a loading control. Top graph depicts band density ratios between pro-caspase 1/vinculin (open bars), and cleaved caspase 1 /vinculin (filled bars).

Figure 3. HAAO blockade decreases atherosclerosis and plasma lipid levels

(A) Schematic overview of the kynurenine pathway and the NCR-631 target 3-hydroxyanthranilic acid 3,4-dioxygenase (HAAO). (B) Twelve-week-old *Ldlr-/-* mice were fed a western diet and treated 3 times weekly with NCR-631 or 3-HAA (200 mg/kg) for 8 weeks. A PBS group was used as control (PBS n=23, NCR-631 n=10, and 3-HAA n=15). *En face* % lesion area in the aortic roots. Pooled data from two independent experiments are shown. Representative micrographs of each group. (C) total cholesterol and (D) triglyceride plasma levels (PBS n=22, NCR-631 n=10, and 3-HAA n=15). (E) Mice body weight at the end of treatment (PBS n=23, NCR-631 n=10, and 3-HAA n=15). * P<0.05; ** P<0.01; Kruskal-Wallis ANOVA with Dunn's post-test. IDO, Indoleamine-2,3-dioxygenase; TDO, tryptophan dioxygenase; KAT, kynurenine aminotransferase; KA, kynurenic acid.

Figure 4. The effects of HAAO blockade in leukocyte infiltration and the inflammasome activation in artery wall

Twelve-week-old *Ldlr-/-* mice were fed a western diet and treated 3 times weekly with NCR-631 (200 mg/kg) or PBS for 8 weeks. (A) Analysis of CD68-positive cell immunostaining in atherosclerotic plaques from NCR-631- or PBS-treated mice (PBS n=9, and NCR-631 n=8). (B) Analysis of CD4-positive immunostaining in atherosclerotic plaques from NCR-631- or PBS-treated mice. Right panels: Right

panels show representative microphotographs. Scale bars = 100 μm. Arrowheads depict CD4+ cells. Data from one independent experiment is shown (PBS n=8, and NCR-631 n=7). (C) Representative western blot analysis of pro- and cleaved-caspase-1 expression in aortas from NCR-631- or PBS-treated mice. Vinculin was used as a loading control. Top graph depicts band density ratios between pro-caspase 1/vinculin (left), and cleaved caspase 1 /vinculin (right). * P<0.05; Mann-Whitney U-test.

Figure 5. HAAO inhibition reduces liver SREBP-2 and HMGCR expression and improves histopathological scores

Analysis of SREBP and target gene mRNA expression in the livers of twelve-week-old *Ldlr-/-* mice fed a western diet and treated 3 times weekly with NCR-631 (200 mg/kg) or PBS. Graphs show the mRNA levels of (A) SREBP-2 (Srebf-2), (B) its target gene Hmgcr. (C) mRNA levels of SREBP-1 (Srebf-1) and (D) its target gene Scd-1. (A-D; PBS n=17, and NCR-631 n=5) *** P<0.001; Mann-Whitney U-test. (E-F) Semiquantitative histopathological examination of the livers. (E) Percentage steatosis grade, hepatocyte ballooning and lobular inflammation in NCR-631 and PBS treated mice. (F) Representative micrographs from haematoxylin and eosin stained samples. Scale Bar = 100 μm. (G) Total cholesterol and (H) triglycerides in livers lipid extracts from NCR-631- or PBS-treated mice are shown (G-H; PBS n=5, NCR-631 n=4). AU = arbitrary units. * P<0.05; Mann-Whitney U-test.

Figure 6. Effects of NCR-613 treatment on LDL-clearance and VLDL output in *Ldlr-/- mice.*

(A) Clearance of injected FITC-LDL (100 μg protein) in *Ldlr–/–* mice treated for 8 weeks with PBS (n=11) or NCR-631 (200 mg/Kg; n=5). Data for each individual were normalized to the fluorescence of plasma taken 1 minute after injection. No significant differences were observed, Two-way ANOVA. (B) Biosynthesis of VLDL was evaluated in *Ldlr–/–* mice that were treated for 8 weeks with PBS (n=4) or NCR-631 (n=5) and injected with tyloxapol to inhibit lipolysis. Data from one independent experiment is shown. Graph shows mean ± SEM plasma triglycerides levels at different times before (0) and after tyloxapol injection. Right side text shows mean ± SEM of triglycerides output rates, and the percentage difference between groups. VLDL = very-low density lipoprotein.

Figure1

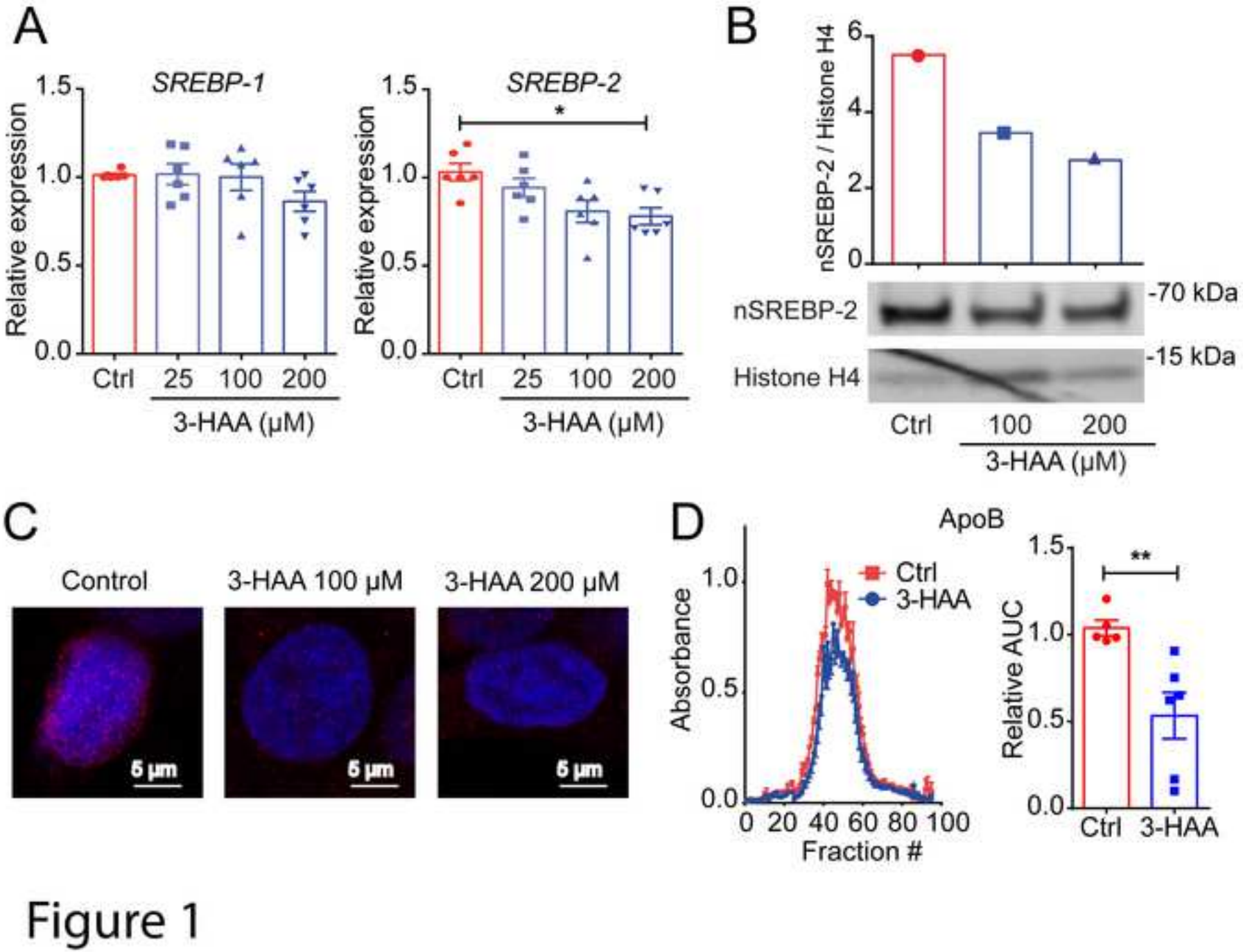

Figure 1

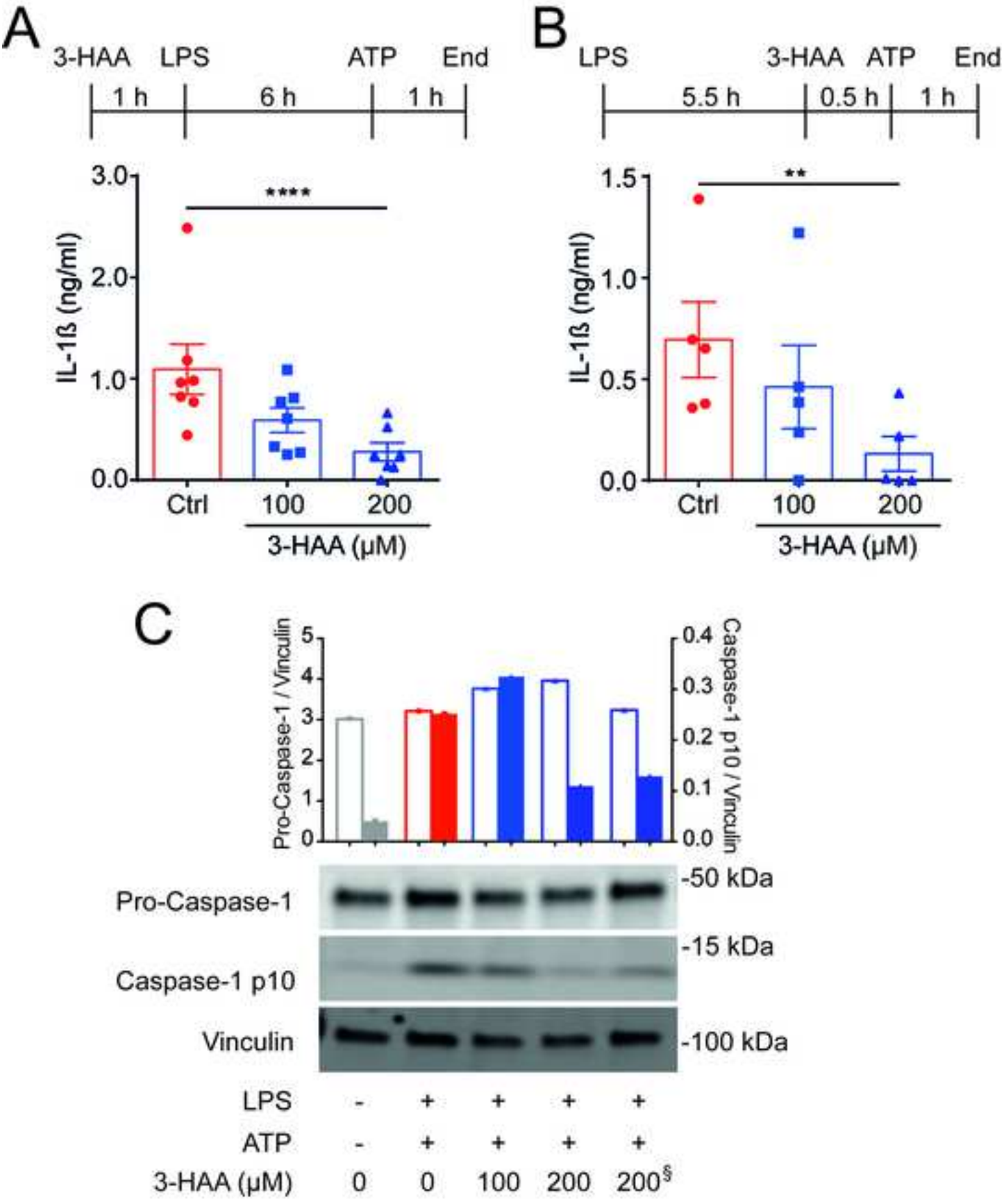

Figure 2

Figure3

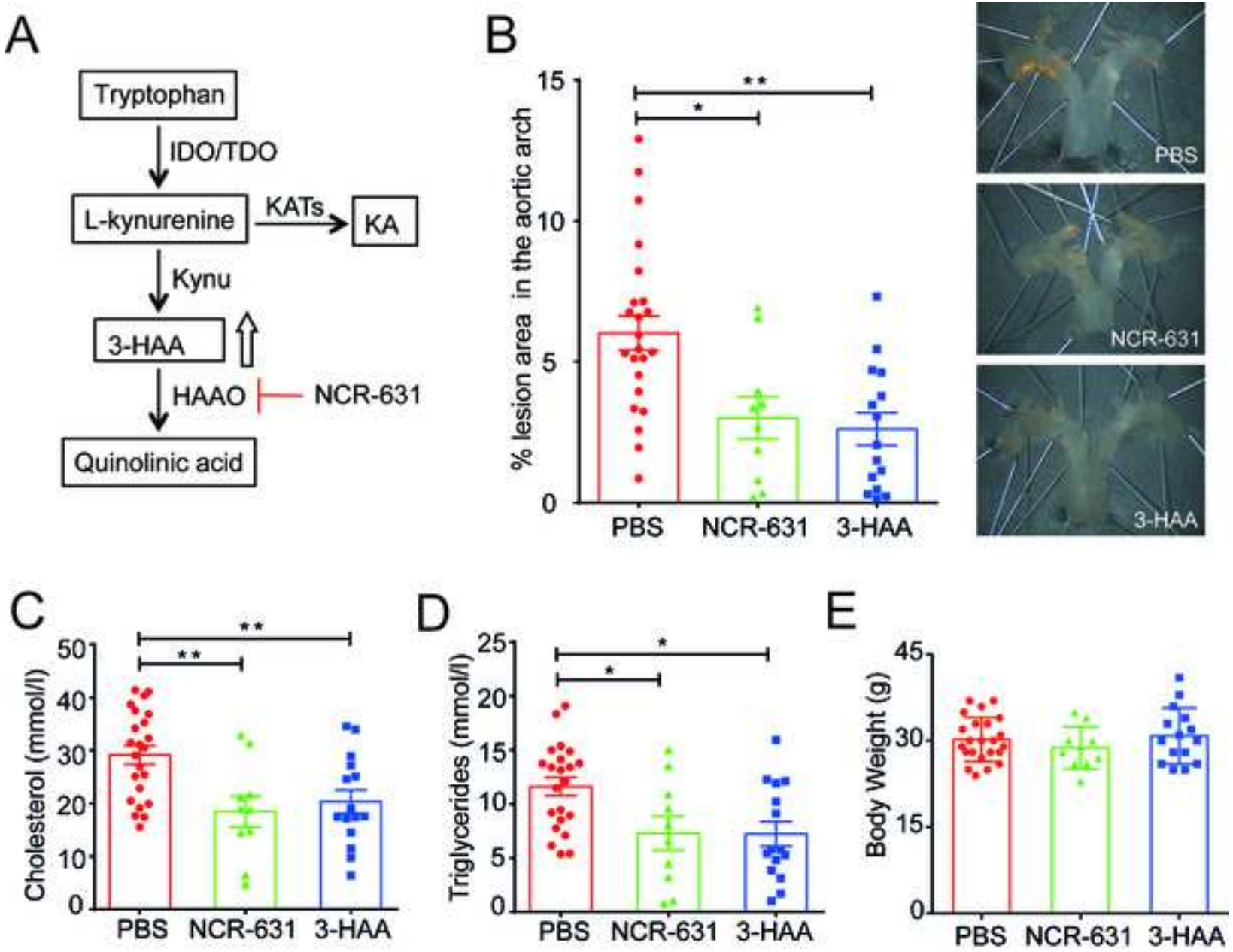

Figure 3

Figure4

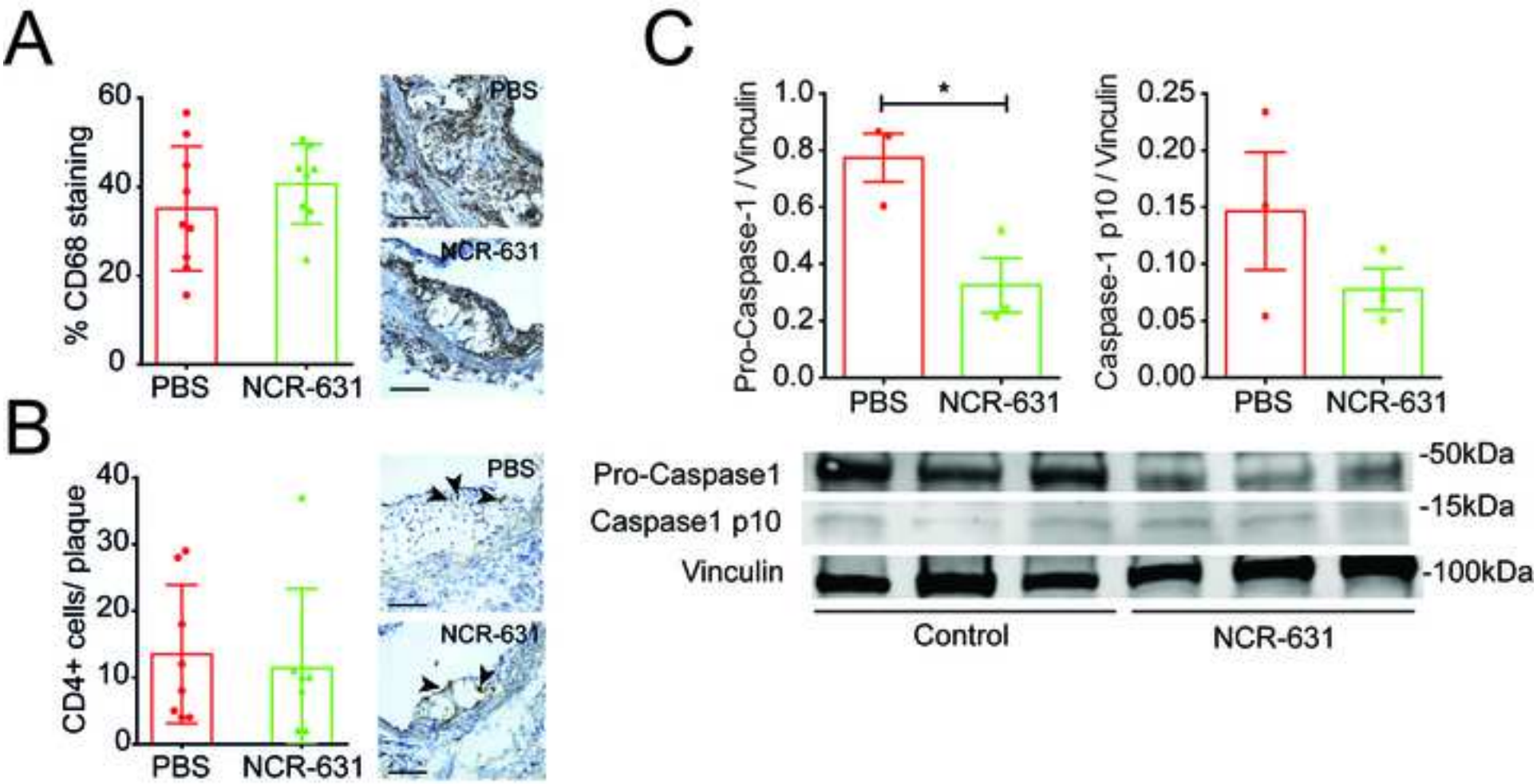

Figure 4

Figure5

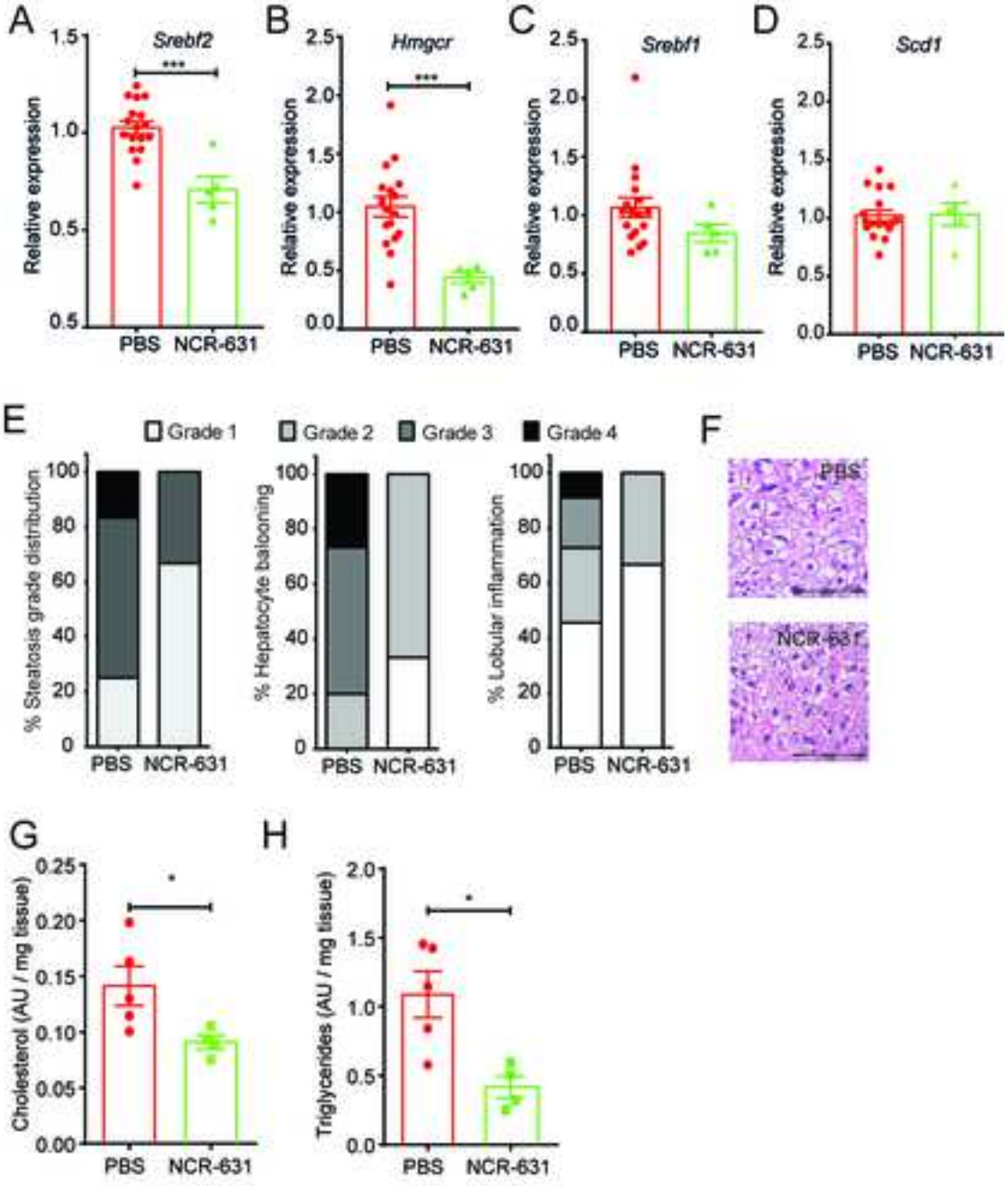

Figure 5

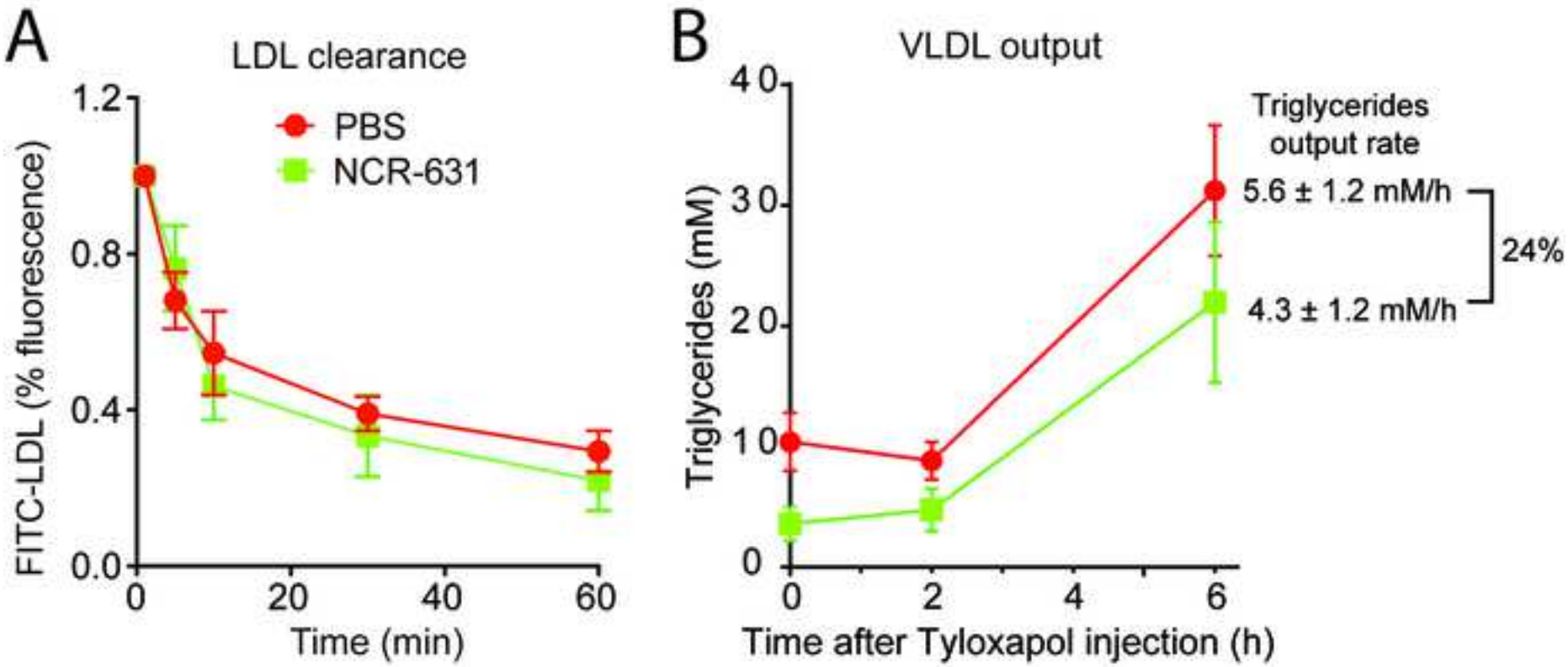

Figure 6